Second-Site Revertants of an Inactive T4 Lysozyme Mutant Restore Activity by Restructuring the Active Site Cleft†

Anthony R. Poteete,‡,§ Sun Dao-Pin,‡ Hale Nicholson,‡ and Brian W. Matthews*,‡

Institute of Molecular Biology, Howard Hughes Medical Institute, and Department of Physics, University of Oregon, Eugene, Oregon 97403, and Department of Molecular Genetics and Microbiology, University of Massachusetts, Worcester, Massachusetts 01655

Received July 10, 1990; Revised Manuscript Received October 9, 1990

ABSTRACT: Substitution of Thr_{26} by Gln in the lysozyme of bacteriophage T4 produces an enzyme with greatly reduced activity but essentially unaltered stability relative to wild type. Spontaneous second-site revertants of the mutant were selected genetically; two of them were chosen for structural and biochemical characterization. One revertant bears (in addition to the primary mutation) the substitution $Tyr_{18} \rightarrow$ His, the other, $Tyr_{18} \rightarrow$ Asp. The primary mutant and both revertant lysozyme genes were reconstructed in a plasmid-based expression system, and the proteins were produced and purified. The two revertant lysozymes exhibit enzymatic activities intermediate between wild type and the primary mutant; both also exhibit melting temperatures approximately 3 °C lower than either the wild type or the primary mutant. Crystals suitable for X-ray diffraction analysis were obtained from both revertant lysozymes, but not the primary mutant. Structures of the double mutant lysozymes were refined at 1.8-Å resolution to crystallographic residuals of 15.1% ($Tyr_{18} \rightarrow$ His) and 15.2% ($Tyr_{18} \rightarrow$ Asp). Model building suggests that the side chain of Gln_{26} in the primary mutant is forced to protrude into the active site cleft, resulting in low catalytic activity. In contrast, the crystal structures of the revertants reveal that the double substitutions (Gln_{26} and His_{18}, or Gln_{26} and Asp_{18}) fit into the same space that is occupied by Thr_{26} and Tyr_{18} in the wild-type enzyme; the effect is a restructuring of the surface of the active site cleft, with essentially no perturbation of the polypeptide backbone. This restructuring is effected by a novel series of hydrogen bonds and electrostatic interactions that apparently stabilize the revertant structures.

The lysozyme of bacteriophage T4 is an especially suitable protein for structural studies. The structure of the wild-type enzyme has been refined to a resolution of 1.7 Å (Weaver & Matthews, 1987; Bell et al., 1990). Moreover, many mutant variants of T4 lysozyme have been found to form isomorphous crystals of high quality; it has thus been possible to examine closely the structural effects of numerous amino acid substitutions in this protein (Matthews, 1987; Alber & Matthews, 1987a).

As an approach to the general problem of how the amino acid sequence of a protein determines its three-dimensional structure, we are attempting to generate informative structural variants of T4 lysozyme by systematic second-site reversion of mutants that abolish lysozyme function. The scheme for generating and selecting such mutants employed in these studies involves four steps: (1) introduction of amber codons into the lysozyme gene borne by a bacteriophage (a P22 hybrid bearing the T4 lysozyme gene in place of its own) that depends on lysozyme function for its ability to form a plaque; (2) testing the amber mutant phage for ability to form plaques on a number of suppressor host strains, each of which inserts a different amino acid in response to the amber codon; (3) selection of plaque-forming revertants in the cases in which the mutant phage fails to form plaques on a particular suppressor strain; and (4) screening among the revertants for second-site revertants by means of a simple genetic test—second-site revertants, unlike primary site revertants, retain the original amber codon and hence are unable to form plaques on a nonsuppressor strain (Knight et al., 1987; Rennell & Poteete, 1989). DNA sequencing of the lysozyme genes of the second-site revertants can suggest which of them might be of interest for structural studies.

In preliminary studies of revertants of missuppressed amber mutants in T4 lysozyme, we identified two revertants that seemed likely, from their sequences and phenotypes, to encode lysozymes with significant, but localized, structural alterations. This paper describes detailed structural studies of these two mutant proteins.

Experimental Procedures

Construction of P22 e416am26 and Isolation of Revertants. Amber codons were introduced via mismatched oligonucleotides into the T4 lysozyme gene borne by plasmid pLH416 (Hardy and Poteete, unpublished experiments) and crossed into phage P22; suppression patterns on bacterial hosts were determined; and second-site revertants were selected and sequenced by methods described previously (Rennell & Poteete, 1989).

Reconstruction of Mutant Lysozyme Genes in an Expression System. Mutations were introduced into the T4 lysozyme gene bearing M13 phage derivative M13 mp18 T4e C54T C97A (Matsumura & Matthews, 1989; Matsumura et al., 1989) according to the method of Kunkel et al. (1987). The T4 lysozyme gene borne by this M13 derivative encodes the "cysteine-less wild-type" mutant C54T C97A. The oligonucleotides employed were 5′-GATGCCAATCTGGTAATAGCC-3′ (T26Q), 5′-TGTGTCTTTATGGATTTTAAG-3′ (Y18H), and 5′-TGTGTCTTTATCGATTTTAAG-3′ (Y18D). (Sequence changes from the wild type are under-

† This work was supported by grants from NIH (GM21967 to B.W.M. and AI24083 to A.R.P.) and by the Lucille P. Markey Charitable Trust. A.R.P. was supported by an NIH research career development award.

‡ University of Oregon.

§ University of Massachusetts.

0006-2960/91/0430-1425$02.50/0

lined; the M13 hybrid contains the strand of the T4 lysozyme gene that is represented in mRNA.) The T26Q alteration was introduced first; a preparation of template bearing it was made and subsequently mutagenized with the two other primers. In each isolate used for further studies, the entire lysozyme gene was sequenced; it was determined that no sequence alterations other than the expected ones were introduced. DNA sequencing was done with Sequenase kits (United States Biochemicals) according to the supplier's protocols.

Mutant T4 lysozyme genes were cut from double-stranded replicative forms of the isolated M13 derivatives with *Bam*H1 and *Hin*dIII and introduced into *Bam*H1- and *Hin*dIII-digested plasmid expression vector pHN1403 by standard methods (Maniatis et al., 1982). *Escherichia coli* strain RR1 was transformed with the mixtures resulting from plasmid construction, and ampicillin-resistant transformants were isolated. Clones bearing the mutant T4 lysozyme genes were identified, grown in liquid culture, and stored at −80 °C after mixing with equal volumes of glycerol. Plasmid pHN1403 is derived from the *lacI*^{Q}-bearing plasmid pHSe5 (Muchmore et al., 1989) by spontaneous deletion of one of its three tandem *tac* promoters and elimination of the *Bam*H1 site between P_{lac} and P_{tac}, (D. Muchmore and A. Roth, personal communication), followed by replacement of the *Bam*H1−*Hin*dIII segment containing the lysozyme gene with the *Bam*H1−*Hin*dIII polylinker segment of M13 mp18.

Lysis Indicator Plate Test. Colonies of *E. coli* strain RR1 bearing plasmids expressing wild-type and mutant lysozymes were stabbed into lysis indicator plates and incubated at 32 °C. The degree of lysis was noted at various times over the subsequent 4–48 h. Lysis indicator plates were prepared from LBH agar plates (10 g of tryptone, 5 g of yeast extract, 5 g of NaCl, 1 mL of 1 M NaOH, and 15 g of agar per liter, with 20 μg/mL thymine added after autoclaving, poured in 100-mm glass Petri dishes) supplemented with ampicillin at 100 μg/mL. These were overlaid with 0.1 mL of 50 mg/mL IPTG and then a mixture of 0.5 mL of a log- or stationary-phase culture of *E. coli* strain RR1 bearing the ampicillin resistance conferring plasmid pCR43 (Muchmore et al., 1989) with 2.5 mL of molten LBH soft agar (as above, but 7 g of agar per liter and no thymine) and incubated at 37 °C for 8–10 h. The bacterial lawns were then subjected to 30–120-s irradiation from a short-wave UV lamp (Mineralight, 4 W, 254 nm) at a distance of approximately 15 cm; 1 mL of chloroform was placed in the lids of the inverted plates, which were left at room temperature for 2–20 h. The plates were stored at 4 °C for up to 1 month.

Purification of Mutant Lysozymes. Strain RR1 bearing lysozyme-producing plasmids was streaked from frozen cultures on LB agar plates (10 g of tryptone, 5 g of yeast extract, 10 g of NaCl, 1 g of glucose, 5 mL of 0.5 M $CaCl_2$, and 15 g of agar per liter) supplemented with ampicillin at 100 μg/mL and incubated at 32 °C for 24 h. Single colonies were used to inoculate 100 mL of LBH broth (10 g of tryptone, 5 g of yeast extract, 5 g of NaCl, and 1 mL of 1 M NaOH per liter) supplemented with ampicillin at 100 μg/mL and simultaneously tested for lysozyme production with lysis plates. The 100-mL cultures were aerated by swirling at 37 °C for 10–12 h and then diluted into 3 L of LB broth (12 g of tryptone, 5 g of yeast extract, 10 g of NaCl, and 1 g of glucose per liter). The 3-L cultures were grown with aeration at 37 °C in a fermentor to an A_{595} of 1.2–1.3, at which point the temperature was reduced to 30 °C and 0.7–0.8 g of IPTG was added. After 1.5 h of continued aeration, little or no lysis was observed in any case; cells were harvested by centrifugation, and supernatants were discarded. Cells from the pellets were resuspended to a volume of 100 mL with lysis buffer (0.1 M sodium phosphate buffer, pH 6.6, 0.2 M NaCl, 10 mM $MgCl_2$, and 1 mM $CaCl_2$); 1 mL of 0.5 M sodium EDTA was added, and the suspension was stirred for 18–20 h at 4 °C. To reduce viscosity, 1 mL of 1 M $MgCl_2$ and a few grains of DNase I were added, and the mixture was stirred for 2 h at room temperature. This procedure resulted in apparently complete lysis of the cells bearing revertant lysozyme-producing plasmids. The primary mutant lysozyme did not lyse the cells as efficiently; in this case, apparently complete lysis was effected by use of a French pressure cell. The lysates were centrifuged for 80 min at 39000*g* to remove debris; supernatants were diluted with water to a conductivity of less than 4 mmho. After testing to ascertain that the pH's of the preparations were in the range 6.5–7.5, they were run under a hydrostatic head of approximately 1.5 m through a 2.5 × 5 cm column of CM-Sepharose, previously equilibrated with 50 mM Tris-HCl, pH 7.25, and 1 mM sodium EDTA; lysozymes were eluted with an 800-mL linear gradient of 50–300 mM NaCl in the same buffer. Peak fractions (identified by absorbance at 280 nm) were pooled, dialyzed against 50 mM sodium phosphate buffer, pH 5.8, and then run through a 1 × 3 cm column of SP Sephadex equilibrated with the same buffer; lysozymes were eluted with SP buffer (100 mM sodium phosphate, pH 6.6, 0.55 M NaCl, and 0.02% sodium azide) and stored in this buffer at 4 °C. Analytical reverse-phase HPLC (Brownlee Aqua Pore RP-300, 2.1 × 30 mm, 0–70% acetonitrile in 0.1% trifluoroacetic acid) of samples of 5–10 μg revealed that each preparation consisted of a single protein species. Yields ranged from approximately 50 to approximately 70 mg. Wild-type (C54T/C97A) lysozyme was purified by similar methods, except that the starting material was the low-speed supernatant of a culture that had lysed after induction of lysozyme.

Activity Measurements. Lysozyme activity was measured by the initial rate of decrease in turbidity (A_{350}) of a suspension of lyophilized *E. coli* in 50 mM Tris-HCl, pH 7.0, starting at an A_{350} of approximately 0.8, as described by Tsugita et al. (1968). Lysozyme concentrations were calculated from A_{280}, assuming that a 1 mg/mL solution of wild-type or primary mutant lysozyme has an A_{280} of 1.28; it was estimated that the replacement of Tyr_{18} by His and Asp in the two revertant proteins would change this value to 1.22. Absolute rates are not reproducible; activities are normalized to a wild-type control.

Stability Measurements. Stability toward heat denaturation was measured essentially as described by Dao-Pin et al. (1990). Proteins in SP buffer were diluted at least 2000-fold, to a concentration of 15–25 μg/mL, in JSB (25 mM KCl and 20 mM potassium phosphate buffer, pH 5.31, aspirated to remove dissolved air). Circular dichroism at 223 nm was monitored as the temperature of the solution was raised from 12 to 80 °C at the rate of 1 °C/min with a Hewlett Packard 89100A thermionic controller interfaced to a Hewlett Packard 87 XM computer. In the cases of all three mutant proteins, denaturation was found to be fully reversible by the restoration of circular dichroism following rapid cooling of the denatured sample from 80 to 12 °C.

Crystallization. Crystals used for X-ray diffraction studies were grown by vapor diffusion in a "sitting drop" configuration. Protein concentrations were adjusted to 15 mg/mL in SP buffer, and 15 μL was mixed with an equal volume of the equilibrating buffer in a well in a sealed chamber containing 0.5 mL of the equilibrating buffer. The buffers were mixtures

of NaH_2PO_4 and K_2HPO_4, in concentrations ranging from 1.6 to 2.2 M (phosphate) and pH's from 6.5 to 7.1; all contained 15 mM 2-hydroxyethyl disulfide. In the cases of the two revertants, crystals were obtained over a 3-week incubation at 4 °C in 2.0 and 2.2 M phosphate at all pH's tested; some that grew in 2.2 M phosphate, pH 6.9 and 7.1, were especially suitable for diffraction, measuring over 0.6 mm along their longer edges. The mutant protein crystals were isomorphous with wild type, space group $P3_221$. No crystals of the primary mutant protein were obtained by this method, or by batch crystallization methods described by Alber and Matthews (1987b).

X-ray Data Collection and Processing. Crystals of the two revertant proteins were equilibrated with a mother liquor consisting of 1.05 M K_2HPO_4, 1.26 M NaH_2PO_4, and 0.23 M NaCl. They were mounted in the beam of a Rigaku Rotaflex RU-200BH rotating anode X-ray generator (graphite-monochromated Cu-K_α radiation at 40 kV × 170 mA). Ten 2° rotation exposures were collected from each of two crystals of each mutant at 4 h per exposure, covering the 30° range of a complete unique data set for each mutant in two overlapping segments, according to the method of Schmid et al. (1981), with data extending to 1.7-Å resolution. Scanning and evaluation of films, scaling of the three films per pack, and scaling/merging of the film packs to a unique data set were as described by Weaver and Matthews (1987).

Refinement. Difference electron density maps ($F_o - F_c$, as well as $2F_o - F_c$) were determined from the observed structure factor amplitudes of the revertant lysozymes in combination with phases and amplitudes calculated from the cysteine-less wild-type structure (Pjura et al., 1990; Bell et al., 1990). The difference density maps were used to guide modeling, which was carried out with an Evans and Sutherland PS330 graphics station, using the program FRODO (Jones, 1982). In modeling the two mutant proteins, it was found that the data were most consistent with the presence of a single molecule of hydroxyethyl disulfide for each pair of neighboring lysozyme molecules related by a 2-fold axis, in effect being "shared" by two lysozyme molecules (not shown). This is one of two common variations that have been observed in crystals of T4 lysozymes; in the other, a larger, overlapping space in the unit cell is occupied by two molecules of hydroxyethyl disulfide (unpublished observations). The resulting structures were refined with the TNT package of restrained least-squares refinement routines (Tronrud et al., 1987).

Results

As part of a systematic study on the effects of single amino acid subsitutions on the function of T4 lysozyme, codon 26 of the lysozyme gene was changed to the amber nonsense codon TAG. The amber mutation was introduced into a hybrid P22 phage, which bears the T4 lysozyme gene in place of its own, and the ability of the resulting mutant phage to form plaques on bacterial strains bearing amber suppressors that insert different amino acids in response to the amber codon was assessed. Previous results have shown that a mutation must reduce lysozyme activity more than 50-fold to reduce the plaque-forming ability of the hybrid phage (Hardy and Poteete, unpublished results). The effects on T4 lysozyme function of substituting four different amino acid residues for Thr_{26} are summarized in Table I. The conservative substitution $Thr_{26} \rightarrow$ Ser has no effect on the plaque-forming ability of the phage, while substitutions of Gln, Tyr, and Leu are all deleterious in varying degree.

Spontaneous revertants of the hybrid phage were selected by plating on the Gln- and Leu-inserting suppressor strains.

Table I: Suppression Patterns of *am26* Phages[a]

	amino acid inserted by bacterial strain[b]				
	none	Ser	Gln	Tyr	Leu
phage[c]					
P22 *e416am26*	–	++	–	±	–
P22 *e416am26 Y18H*	–	++	++	+	+
P22 *e416am26 Y18H R*[d]	–	++	++	+	+
P22 *e416am26 Y18D*	–	+/++[e]	+	+	+
P22 *e416am26 Y18D R*[d]	–	+/++[e]	+	+	+

[a] (++) large plaques; (+) tiny plaques, high efficiency of plating; (±) tiny plaques, low efficiency of plating; (–) no plaque formation above the frequency of reversion. [b] Suppressor strains of *Salmonella typhimurium* described previously (Rennell & Poteete, 1989). [c] All phages shown bear, in addition to the *am26* allele, an additional mutation that results in the substitution $Val_{57} \rightarrow$ Ala in T4 lysozyme. This mutation was inadvertently introduced during the construction of P22 *e416am26*; it is not present in the purified lysozymes used in subsequent experiments. [d] The notation *R* designates reconstructed phages in which the T4 lysozyme genes borne by revertant phages were introduced into otherwise wild-type P22 *e416*. [e] The designation "+/++" is used to indicate plaques that, while not describable as "tiny", were reproducibly smaller than those designated "++".

Table II: Activity and Stability of Mutant Lysozymes

protein	% of wild-type activity	T_m (°C)
wild type	100	65.3
T26Q	1.9	64.4
T26Q/Y18H	4.7	61.9
T26Q/Y18D	13	61.3

It was found that slightly over half of the revertants were unable, like the parent phage, to form plaques on a non-amber suppressor strain and hence were likely to retain the original amber mutation and bear in addition a second-site compensating mutation in T4 lysozyme. The suppression patterns of two of the revertant phages are shown in Table I; these two, selected for further study, will henceforth be designated by abbreviations indicating the nature of the mutations they bear: T26Q/Y18H (for $Thr_{26} \rightarrow Gln/Tyr_{18} \rightarrow$ His) and T26Q/Y18D (for $Thr_{26} \rightarrow Gln/Tyr_{18} \rightarrow$ Asp). In terms of conferring plaque-forming ability, it can be seen that Y18H and Y18D improve the function of lysozymes bearing substitutions of Gln, Tyr, and Leu at position 26. Two differences between the second-site mutants can be seen: Y18H appears to help more than Y18D when the amino acid residue at position 26 is Gln; and Y18D, but not Y18H, impairs the function of lysozyme bearing the substitution of Ser for Thr_{26}.

In further studies to characterize the two revertant lysozymes (data not shown), the DNA sequence alterations of Y18H and Y18D were determined. In addition, the T4 lysozyme genes were cut out of the revertant phages and reintroduced into an otherwise wild-type hybrid phage. As indicated in Table I, the reconstructed phages' suppression patterns were identical with those of the original revertants, indicating that the differences in plating phenotype between the parent and revertant phages were indeed due to differences in their lysozyme genes.

For structural studies, mutations corresponding to T26Q, Y18H, and Y18D were introduced into a plasmid that directs the synthesis of large amounts of the cysteine-less pseudo-wild-type lysozyme C54T C97A (Matsumura & Matthews, 1989; Pjura et al., 1990). Three mutant lysozymes were produced: the primary mutant (T26Q) and the two revertants (T26Q/Y18H and T26Q/Y18D).

Purified pseudo-wild-type, primary mutant, and revertant lysozymes were tested for activity and thermal stability, with the results indicated in Table II. The primary mutation has

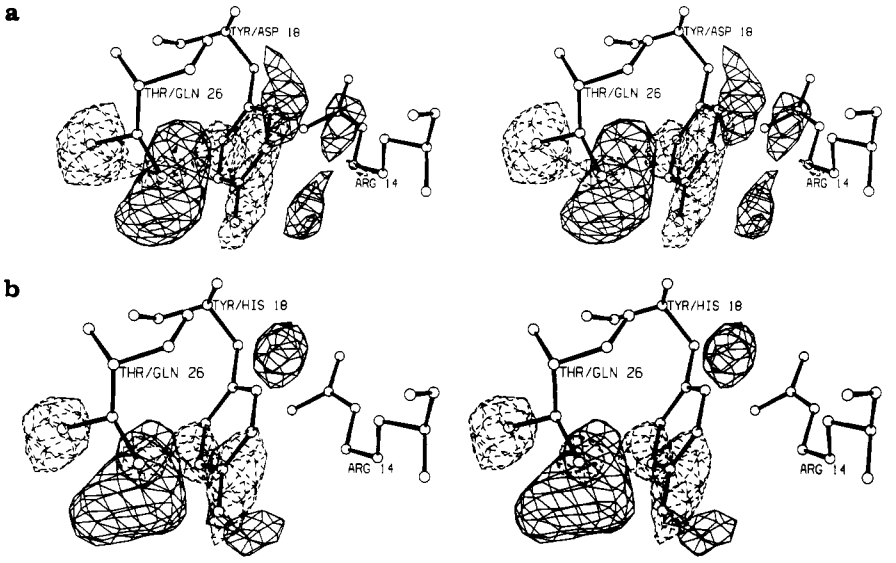

FIGURE 1: Stereo drawings of difference electron density maps between revertants T26Q/Y18H (a) and T26Q/Y18D (b) and pseudo wild type in the vicinity of the altered residues, superimposed on residues Arg_{14}, Tyr_{18}, and Thr_{26} of the pseudo-wild-type protein. The difference electron density is calculated with amplitudes equal to the difference between the observed structure amplitudes of the mutant and pseudo-wild-type proteins, and phases are calculated from the refined pseudo-wild-type (cysteine-less) structure. Resolution is 1.8 Å. The negative density (broken lines) and positive density (solid lines) are contoured at $\pm 4.4\sigma$, where σ is the root-mean-square difference density throughout the mapped part of the unit cell.

little effect on the thermal stability of the protein, reducing T_m by only 0.9 °C at pH 5.3; the two revertant lysozymes exhibit slightly lower values of T_m, 3.4 °C (T26Q/Y18H) and 4.0 °C (T26Q/Y18D) below that of wild type. In contrast, the effects of the mutations on enzymatic activity are substantial. The primary mutation reduces the specific activity (relative to wild type) over 50-fold; the secondary mutations increase this by factors of 2.5 (T26Q/Y18H) and 6.8 (T26Q/Y18D).

Crystals of the two revertants, but not the primary mutant, were obtained and used in X-ray diffraction studies as described under Experimental Procedures. Difference electron density maps between the two mutants and wild type reveal two main features: (1) large negative and positive peaks in the immediate vicinity of the side chains of the residues that are substituted in the mutants (shown in Figure 1) and (2) a lack of prominent peaks elsewhere, indicating relatively little change in the overall structure, in particular, no movement of the polypeptide backbone.

Models of the two revertant lysozymes were built and refined to crystallographic residuals of 15.1% (T26Q/Y18H) and 15.2% (T26Q/Y18D) at 1.8-Å resolution. Statistics relating to the structure determinations are given in Table III. Two aspects of the model building were not completely obvious from the initial difference density maps. First, in both cases, the electron density was consistent with either of two different Gln_{26} rotamers, in which the positions of the ϵ-carbon and nitrogen atoms are exchanged. Models built with either of the two rotamers, $\chi_3 = 18°$ or $-162°$, refine to the same crystallographic residuals. However, setting $\chi_3 = -162°$ in the T26Q/Y18H mutant gives final refined values of 14.5 and 29.8 Å^2 for the temperature factors of NE2 and OE1, respectively, while setting $\chi_3 = 18°$ gives corresponding values of 20.9 and 21.0 Å^2. One interpretation of this difference is that it is what one might expect if the temperature factors of the two atoms were in fact nearly equal. Then, in the incorrect conformation, refinement would lead to an overestimate of the temperature factor of the oxygen atom (interpreted as the smaller nitrogen) and a corresponding underestimate of the temperature factor of the nitrogen. A similar result is seen in a comparison of the two rotamers in T26Q/Y18D. The rotamers that generate nearly equal temperature factors are incorporated into both structures ($\chi_3 = 18°$ in T26Q/Y18H, 15° in T26Q/Y18D). The second nonobvious modeling feature concerned Arg_{14} in the T26Q/Y18D revertant. In this case, the initial $2F_o - F_c$ density map did not indicate where the side chain should be placed, beyond the β-carbon. To locate this side chain, it was necessary to commence refinement with an alanine at this position, produce an intermediate $2F_o - F_c$ density map (in which the placement of the side chain was more obvious), build the Arg_{14} side chain into the model, and then complete the refinement. The position occupied by the side chain of Arg_{14} in T26Q/Y18D differs substantially from that in T26Q/Y18H and wild type. This conformational change is apparently promoted by a favorable electrostatic interaction between Arg_{14} and Asp_{18} in the T26Q/Y18D

Table III: Crystallographic Statistics

	protein	
	T26Q/Y18H	T26Q/Y18D
Data Collection		
cell dimensions		
a, *b* (Å)	61.0	61.1
c (Å)	96.8	96.6
unique reflections		
observed	14077	14184
used	13392	13404
% of complete set	67	67
R_{merge} (%)	4.7	5.9
Refinement		
R (%)	15.1	15.2
Δ_{bond} (Å)	0.021	0.022
Δ_{angle} (deg)	2.7	3.1

[a] Unique reflections used are the subset of the total observed that fell within the resolution range 6.0–1.8 Å and could be matched with expected reflections by the data processing program. R_{merge} is a measure of the residual discrepancy between intensities of the same reflection measured on different films, after scaling. *R* is the crystallographic residual following refinement to 1.8-Å resolution. Δ_{bond} and Δ_{angle} are the root-mean-square discrepancies of the values of the bond lengths and angles between the refined structures and "ideal" values derived from crystallographic studies of small molecules (Tronrud et al., 1987).

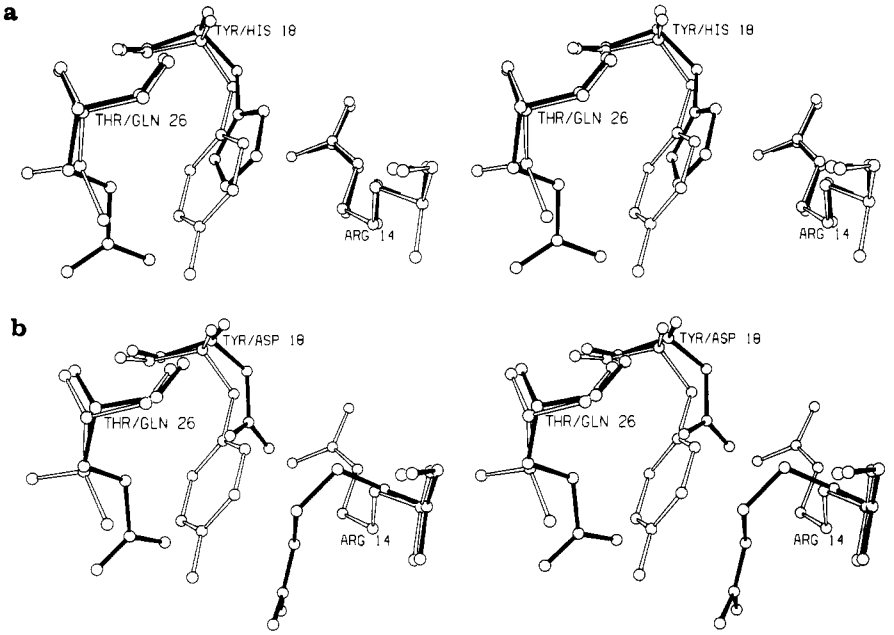

FIGURE 2: Stereo drawings of residues 14, 18, and 26 from cysteine-less wild type (open bonds) superimposed on the corresponding residues of T26Q/Y18H (a) and T26Q/Y18D (b) revertant lysozymes (solid bonds) following refinement.

structure. The structures of the mutant lysozymes are compared with that of the wild type in the vicinity of the altered residues in Figure 2.

In the absence of X-ray diffraction data on the primary mutant, computer modeling was employed to ascertain whether Gln_{26} could be accommodated by the wild-type structure without steric clashes or loss of stabilizing interactions. That this might well be the case is suggested by the lack of any significant effect of the primary mutation on the overall stability of the protein. A hypothetical model structure of the primary mutant is shown in Figure 3. In it, Gln_{26} makes apparently favorable contacts with Tyr_{18} and the polypeptide backbone, in a way that does not appear to require any movement of either; indeed, the model shown is the only stereochemically reasonable one we could find that did not require such movement. It will be noticed, however, that this model-built conformation of Gln_{26} (Figure 3b) is not the same as that in the observed structures of the revertants (Figure 3c,d). In the revertants the side chain is folded away from the active site cleft ($\chi_1 \sim 80°$), whereas in the presumed primary mutant the extra atoms resulting from the Thr → Gln substitution protrude into the active site cleft ($\chi_1 \sim 180°$).

Discussion

The mutant T4 lysozymes characterized in these studies differ from wild type substantially in activity, and only slightly in stability, the reverse of what has been the case in most of the other T4 lysozyme variants whose structures have been solved [e.g., see Alber et al. (1986)]. The structural alterations found in the two revertant lysozymes have the effect of altering the surface of the active site cleft. Inspection of these structures suggests a simple explanation for the effects of the amino acid substitutions on activity: In the primary mutant the side chain of Gln_{26} appears to protrude into the active site cleft, interfering with the binding of substrate. Substitution of Tyr_{18} with His or Asp allows Gln_{26} to rotate away from the active site cleft and to pack more toward the interior of the protein, partially alleviating the substrate-binding problem. These notions are illustrated in Figure 3, which shows cross sections of the active site clefts of the wild-type and mutant lysozymes.

The structure of the primary mutant shown in Figure 3b is hypothetical, based on model building. In the absence of X-ray data, it is difficult to assess the validity of this structure. However, it is clear from inspection of the structures of the other proteins that Gln_{26} could not have the same conformation in the primary mutant and the revertants unless Tyr_{18} is substantially displaced from its wild-type position, as the two residues would otherwise overlap spatially. Substantial displacement of Tyr_{18} in the primary mutant, in turn, seems unlikely. Tyr_{18} engages in van der Waals interactions with surrounding residues, and its displacement might be expected to destabilize the protein. The stability data (Table II) provide indirect support for these assumptions. The primary mutation, Thr_{26} → Gln, reduces the melting temperature by only 0.9 °C, suggesting that Tyr_{18} retains its wild-type position. The secondary mutations Tyr_{18} → His and Tyr_{18} → Asp reduce the melting temperature by 2.5–3.1 °C, suggesting that the conformation of Tyr_{18} is, indeed, stabilized by a number of favorable interactions that are lost, or partially lost, when Tyr_{18} is replaced with a smaller residue.

The data in Table I suggest that the Tyr_{18} → Asp substitution, which increases the activity of lysozyme bearing Gln_{26}, actually decreases the activity of a lysozyme bearing the conservative substitution Thr_{26} → Ser. Evidently, the Tyr_{18} → Asp substitution is deleterious in a normal, or near-normal, context, but helpful in another. These observations can be rationalized by assuming that the Tyr_{18} → Asp replacement perturbs both the Thr_{26} → Ser and the Thr_{26} → Gln structures, but in different ways. The Thr_{26} → Ser structure is presubably very similar to wild type, and in this case the Tyr_{18} → Asp substitution perturbs the wild-type-like structure, causing a reduction in activity. In the case of the Thr_{26} → Gln structure, however, it is presumed that the subsequent Tyr_{18} → Asp substitution allows the side chain of Gln_{26} to move out of the active site cleft. Thus, in this case the change in conformation is toward that of wild type, resulting in an increase in activity.

The data in Table I also indicate that the lysozyme with the Thr_{26} → Tyr replacement is more active than Thr_{26} → Gln or Thr_{26} → Leu. Model building suggests that a tyrosine at position 26 cannot be placed in a position analogous to that assumed for Gln_{26} (Figure 3b), i.e., with $\chi_1 \sim 180°$, because

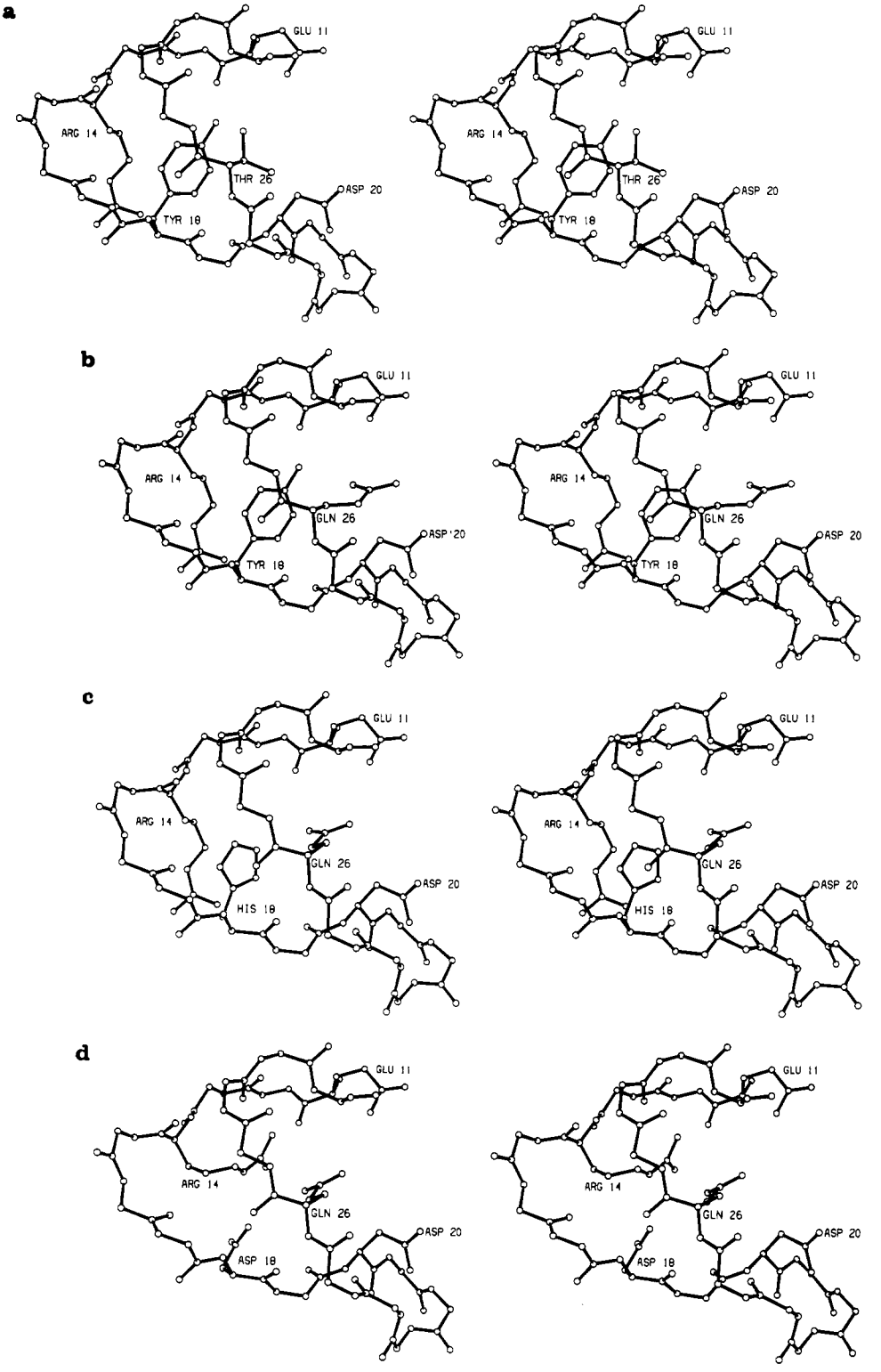

FIGURE 3: Stereo drawings of wild-type and mutant lysozymes, showing a cross section of the active site cleft, bounded at top and bottom by Glu_{11} and Asp_{20}, the key catalytic residues. (a) Wild type; (b) the primary mutant T26Q, hypothetical structure based on model building; (c) revertant T26Q/Y18H; (d) revertant T26Q/Y18D.

the phenolic hydroxyl would sterically clash with Glu_{11}. Rather, it seems that a tyrosine at position 26 would probably adopt a conformation with $\chi_1 \sim -80°$ and the plane of the phenolic side chain approximately parallel to the carboxylate of Asp_{20} (Figure 3b). In contrast to Gln_{26}, which is presumed to protude directly into the active site cleft, Tyr_{26} would therefore be aligned along the side of the cleft and so interfere less with catalytic activity. By the same token, the subsequent replacements $Tyr_{18} \rightarrow$ His and $Tyr_{18} \rightarrow$ Asp would not create sufficient space to allow the bulky side chain of Tyr_{26} to rotate out of the active site cleft and so would be expected to be poor suppressors of the $Thr_{26} \rightarrow$ Tyr replacement, as is observed (Table I). While model building suggests that the $\chi_1 \sim -80°$ conformation is possible for a tyrosine at position 26, the different shape of the glutamine side chain seems to restrict its conformation to $\chi_1 \sim 180°$, as noted above.

In the case of a leucine at position 26, model building in the context of wild-type lysozyme suggests that one or other of the two γ-methyl groups will protrude into the active site, explaining the substantial loss of activity for this variant (Table

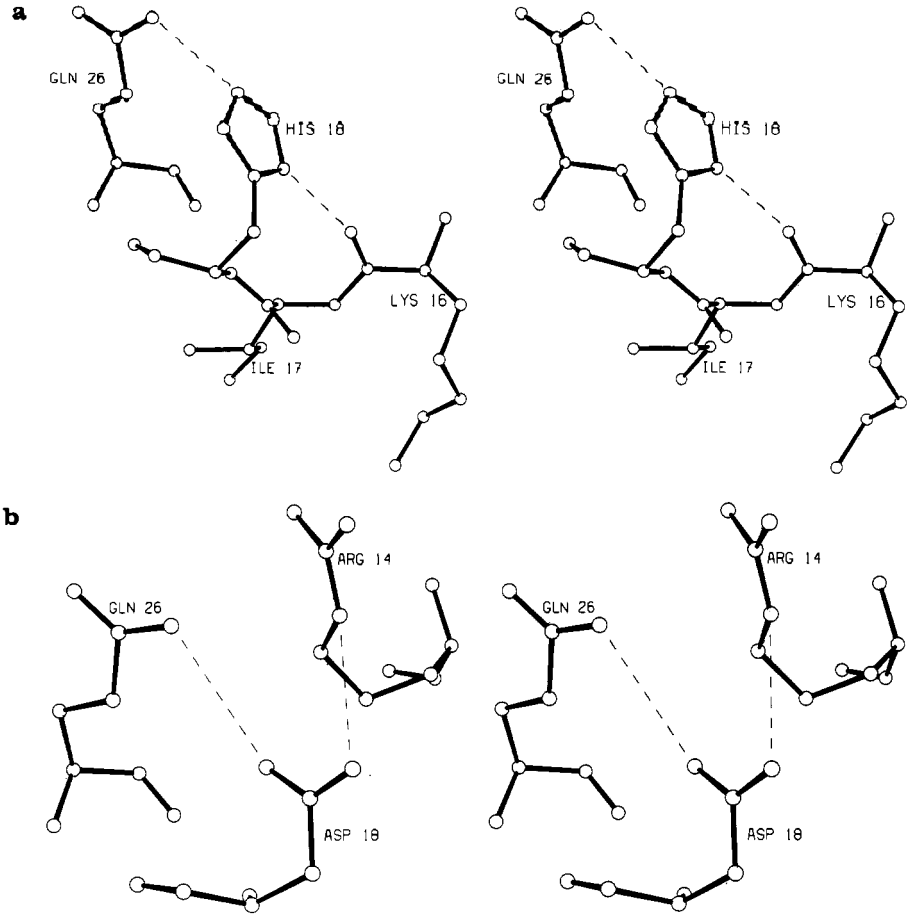

FIGURE 4: Stereo drawings of residues in the revertant lysozymes, illustrating inferred new intramolecular interactions. (a) T26Q/Y18H. Interatomic distances are as follows: $Gln_{26}N_{\epsilon 2}$–$His_{18}N_{\epsilon 2}$, 2.8 Å; $His_{18}N_{\delta 1}$–$Lys_{16}O$, 2.6 Å. (b) T26Q/Y18D. Interatomic distances are as follows: $Gln_{26}N_{\epsilon 2}$–$Asp_{18}O_{\delta 2}$, 3.4 Å; $Asp_{18}O_{\delta 1}$–$Arg_{14}N_{\epsilon}$, 3.4 Å.

I). The subsequent $Tyr_{18} \rightarrow His$ or $Tyr_{18} \rightarrow Asp$ replacement allows Leu_{26} to rotate at least partly out of the active site cleft and so provide partial suppression of the Leu_{26} phenotype (Table I). In this context it is of interest to note in both the T26Q/Y18D and T28Q/Y18H revertant lysozyme structures that the position adopted by Gln_{26} is determined at least in part by hydrogen-bonding interactions with Asp_{18} or His_{18} (Figure 4). It suggests that the reverting mutation may do more than passively allow the side chain of Gln_{26} to move away from Glu_{11}; rather, His_{18} and Asp_{18} may play a more active role in pulling the side chain of Gln_{26} away from the active site cleft.

An unexplained aspect of the activities of the mutant proteins concerns their rank order. Data in Table I indicate that the T26Q/Y18H revertant works better in vivo than T26Q/Y18D when Gln is inserted in response to the amber codon at position 26. Moreover, in the lysis indicator plate assay described under Experimental Procedures, T26Q/Y18H makes more prominent halos than T26Q/Y18D (not shown). However, the T26Q/Y18D revertant lysozyme exhibits a higher specific activity in vitro than T26Q/Y18H (Table II). Plausible interpretations of these observations include the following: (1) activity in vitro does not precisely mirror function in vivo; (2) the purified preparation of Y18H may not have been fully active.

Inspection of the structures of the revertant lysozymes suggests that the small changes in stability accompanying the double substitutions are due to a near canceling-out of relatively large stabilizing and destabilizing factors. In the case of T26Q/Y18H, a hydrogen bond involving the threonine hydroxyl and the polypeptide backbone is lost, along with favorable interactions involving close packing between the hydrophobic surfaces of Tyr_{18} and its neighbors (not shown). These losses are partially compensated by the acquisition in the double mutant of two new intramolecular hydrogen bonds, one between His_{18} and a backbone carbonyl oxygen, the other between N_{ϵ} of His_{18} and the amide group of Gln_{26}. We surmise that the latter interaction involves $N_{\epsilon 2}$ of Gln_{26} and unprotonated N_{ϵ} of His_{18}, for two reasons: as described under Results, the corresponding Gln_{26} rotamer fits the diffraction data better; and the pK_a of His_{18}, measured by nuclear magnetic resonance spectroscopy, is 6.3 ± 0.052 (E. Anderson, personal communication), consistent with its being largely unprotonated at pH 6.9–7.1 in the crystals. These new interactions are shown in Figure 4A. Similarly, in T26Q/Y18D, two new favorable interactions appear: a hydrogen bond between Asp_{18} and Gln_{26} and a salt bridge between Asp_{18} and Arg_{14} (Figure 4b). Arg_{14} in this mutant (but not in T26Q/Y18H) is rotated considerably from its position in wild type (see Figure 3c,d).

ACKNOWLEDGMENTS

We thank Larry Hardy for providing P22*e416am26*, Joan Wozniak for technical assistance, Walter Baase for guidance in thermal denaturation measurements and comments on the manuscript, and Eric Anderson for measuring the pK_a of His_{18} in T26Q/Y18H. A.R.P. thanks Keith Wilson, Dale Tronrud, Larry Weaver, Rick Faber, Steve Roderick, and Elisabeth Eriksson for advice on X-ray data collection, processing, and refinement.

Registry No. Gln, 56-85-9; His, 71-00-1; Asp, 56-84-8; Thr, 72-19-5; Tyr, 60-18-4; lysozyme, 9001-63-2.

REFERENCES
Alber, T., & Matthews, B. W. (1987a) in *Protein Engineering*, pp 289-297, Alan R. Liss, New York.
Alber, T., & Matthews, B. W. (1987b) *Methods Enzymol. 154*, 511-533.
Alber, T., Grutter, M. G., Gray, T. M., Wozniak, J. A., Weaver, L. H., Chen, B.-L., Baker, E. N., & Matthews, B. W. (1986) in *ULCA Symposia on Molecular and Cellular Biology, New Series*, Vol. 39, pp 307-318, Alan R. Liss, New York.
Bell, J. A., Wilson, K. P., Zhang, X.-J., Faber, H. R., Nicholson, H., & Matthews, B. W. (1990) *Proteins: Struct., Funct. Genet.* (in press).
Dao-Pin, S., Baase, W. A., & Matthews, B. W. (1990) *Proteins: Struct., Funct. Genet. 7*, 198-204.
Jones, T. A (1982) in *Crystallographic Computing* (Sayre, D., Ed.) pp 303-317, Oxford University Press, Oxford, U.K.
Knight, J. A., Hardy, L. W., Rennell, D., Herrick, D., & Poteete, A. R. (1987) *J. Bacteriol. 169*, 4630-4636.
Kunkel, T. A., Roberts, J. D., & Zakour, R. A. (1987) *Methods Enzymol. 154*, 367-382.
Maniatis, T., Fritsch, E. F., & Sambrook, J. (1982) *Molecular Cloning: A Laboratory Manual*, Cold Spring Harbor Laboratory, Cold Spring Harbor, NY.
Matsumura, M., & Matthews, B. W. (1989) *Science 243*, 792-794.
Matsumura, M., Signor, G., & Matthews, B. W. (1989) *Nature 342*, 291-293.
Matthews, B. W. (1987) *Biochemistry 26*, 6885-6888.
Muchmore, D. C., McIntosh, L. P., Russell, C. B., Anderson, D. E., & Dahlquist, F. W. (1989) *Methods Enzymol. 177*, 44-73.
Pjura, P. E., Matsumura, M., Wozniak, J. A., & Matthews, B. W. (1990) *Biochemistry 29*, 2592-2598.
Rennell, D., & Poteete, A. R. (1989) *Genetics 123*, 431-440.
Schmid, M. R., Weaver, L. H., Holmes, M. A., Grutter, M. G., Ohlendorf, D. H., Reynolds, R. A., Remington, S. J., & Matthews, B. W. (1981) *Acta Crystallogr., Sect. A A37*, 701-710.
Tronrud, D. E., Ten Eyck, L. F., & Matthews, B. W. (1987) *Acta Crystallogr., Sect. A. A43*, 489-503.
Tsugita, A., Inouye, M., Terzaghi, E., & Streisinger, G. (1968) *J. Biol. Chem. 243*, 391-397.
Weaver, L. H., & Matthews, B. W. (1987) *J. Mol. Biol. 193*, 189-199.

Role of the Conserved Active Site Residue Tryptophan-24 of Human Dihydrofolate Reductase As Revealed by Mutagenesis†

William A. Beard,‡ James R. Appleman,‡ Shaoming Huang,§ Tavner J. Delcamp,§ James H. Freisheim,§ and Raymond L. Blakley*,‡,∥

Department of Biochemical and Clinical Pharmacology, St. Jude Children's Research Hospital, Memphis, Tennessee 38101, Department of Biochemistry, Medical College of Ohio, Toledo, Ohio 43699, and Department of Pharmacology, University of Tennessee College of Medicine—Memphis, Memphis, Tennessee 38163

Received May 29, 1990; Revised Manuscript Received September 17, 1990

ABSTRACT: The active sites of all bacterial and vertebrate dihydrofolate reductases that have been examined have a tryptophan residue near the binding sites for NADPH and dihydrofolate. In cases where the three-dimensional structure has been determined by X-ray crystallography, this conserved tryptophan residue makes hydrophobic and van der Waals interactions with the nicotinamide moiety of bound NADPH, and its indole nitrogen interacts with the C^4 oxygen of bound folate through a bridge provided by a bound water molecule. We have addressed the question of why even the very conservative replacement of this tryptophan by phenylalanine does not seem to occur naturally. Human dihydrofolate reductase with this replacement of tryptophan by phenylalanine has increased rate constants for dissociation of substrates and products and a considerably decreased rate of hydride transfer. These cause some changes in steady-state kinetic behavior, including substantial increases in Michaelis constants for NADPH and dihydrofolate, but there is also a 3-fold increase in k_{cat}. The branched mechanistic pathway for this enzyme has been completely defined and is sufficiently different from that of wild-type enzyme to cause changes in some transient-state kinetics. The most critical changes resulting from the amino acid substitution appear to be a 50% decrease in stability and a decrease in efficiency from 69% to 21% under intracellular conditions.

Among amino acid residues at the active site of dihydrofolate reductase (DHFR)[1] are several that are conserved in all the known sequences of the enzyme from vertebrate species. Although bacterial DHFRs have structures congruent with the vertebrate enzyme, their sequence homology with vertebrate DHFR is quite low. Nevertheless, some of these active site residues are conserved in bacterial DHFR sequences as

† This work was supported in part by U.S. Public Health Service Research Grants R01 CA 31922 (R.L.B.) and R01 CA 41461 (J.H.F.), Cancer Core Grant P30 CA 21765 (R.L.B.), and U.S. Public Health Service Training Grant 5 T32 CA 09346 (W.A.B.) from the National Cancer Institute, National Institutes of Health, and by the American Lebanese Syrian Associated Charities (R.L.B., W.A.B., and J.R.A.).

‡ St. Jude Children's Research Hospital.
§ Medical College of Ohio.
∥ University of Tennessee College of Medicine—Memphis.

[1] Abbreviations: DHFR, dihydrofolate reductase; ecDHFR, *Escherichia coli* DHFR; lcDHFR, *Lactobacillus casei* DHFR; rhDHFR, recombinant human DHFR; H_2folate, 7,8-dihydrofolate; H_4folate, (6*S*)-5,6,7,8-tetrahydrofolate; MATS, 25 mM MES, 25 mM acetate, 50 mM Tris, 100 mM NaCl, and 0.02% sodium azide; MTX, methotrexate; NADPD, (4*R*)-[^{2}H]NADPH; MES, 2-(*N*-morpholino)ethanesulfonic acid; Tris, tris(hydroxymethyl)aminomethane; wt, wild type; W24F, mutant rhDHFR with $Trp^{24} \rightarrow Phe$. $k_{cat} = V_{max}/[E]$, where V_{max} is the steady-state maximum velocity and [E] is the enzyme concentration.

0006-2960/91/0430-1432$02.50/0